Transducing chemical energy through catalysis by an artificial molecular motor

Peng-Lai Wang[1,2], Stefan Borsley[1], Martin J. Power[1], Alessandro Cavasso[3], Nicolas Giuseppone[3,4*], David A. Leigh[1,2*]

[1]Department of Chemistry, University of Manchester, Manchester M13 9PL, UK.

[2]School of Chemistry and Molecular Engineering, East China Normal University, Shanghai, China.

[3]SAMS Research Group, Université de Strasbourg, Institut Charles Sadron – CNRS, 23 rue du Loess, BP 84047, 67034 Strasbourg Cedex 2, France

[4]Institut Universitaire de France (IUF), Paris 75005, France

*Correspondence to: david.leigh@manchester.ac.uk, giuseppone@unistra.fr

Cells display a range of mechanical activities enabled by the cytoskeleton, a viscoelastic hydrogel manipulated by motor proteins powered through catalysis.[1] This raises the question of how the acceleration of a chemical reaction can enable the energy released from that reaction to be transduced, and thereby work to be done, by a molecular catalyst.[2–7] Here we demonstrate the molecular-level transduction of chemical energy to mechanical force[8,9] in the form of the powered contraction and powered re-expansion of a crosslinked polymer gel driven by the directional rotation of embedded artificial catalysis-driven[10] molecular motors. Continuous 360° rotation of the rotor about the stator of motor-molecules incorporated within the polymeric framework of the gel, twists the polymer chains of the crosslinked network around one another (either clockwise or anti-clockwise, depending on the chirality of the fuelling system). This progressively increases writhe and tightens entanglements, causing macroscopic contraction of the gel to ~70% of its original volume. The limit of contraction corresponds to the stall force of the motor;[2–4] the point at which, despite catalysis continuing, the untwisting force exerted by the entwined strands balances conformation selection in the motor's catalytic cycle. Subsequent addition of the opposite enantiomeric fuelling system powers rotation of the motor-molecules of the contracted gel in the reverse direction, unwinding the entanglements and causing the gel to re-expand. Continued powered twisting of the strands in the new direction causes the gel to contract once again. The experimental demonstration of work against a load by a synthetic catalyst, and the mechanism of the transduction of energy by a catalyst through kinetic asymmetry[14–16] in its acceleration of a fuel-to-waste reaction, informs both the debate[3,5,7] surrounding the mechanism of force generation by biological motors and the design principles[6,11–16] for artificial molecular nanotechnology.

All biomolecular motors are catalysts.[1] They transduce energy from the fuel-to-waste reaction they catalyse—generally adenosine triphosphate (ATP) to adenosine diphosphate (ADP) plus inorganic phosphate (P_i)—to power the diverse array of tasks required by the cell, including transport, synthesis

and force generation. Motor proteins are exquisitely complex, making it difficult to provide fundamental answers to how the action of catalysis causes the energy from an accelerated reaction to be transduced.[1] Although a power stroke (a large amplitude viscoelastic conformational change[2–5]) occurs during the mechanism of myosin, the force-generating motor protein in muscle,[8,9] it is contested[3,5] whether a power stroke is even necessary for force generation by molecular machines.

Artificial molecular motors[17–24] and pumps[25–34] can provide insights regarding the mechanisms of powered molecular-level motion.[13–16] Molecular machines have been interfaced with other components to perform tasks,[29,32,35–38] including the use of light-driven rotary motors to disrupt cell membranes[35] and drive the contraction of gels.[36–38] However, performing work with artificial catalysis-driven molecular motors, the synthetic analogues of motor proteins, has remained elusive.

A biaryl molecular rotary motor that operates through its organocatalysis of a fuel-to-waste reaction was recently reported.[10] The motor-molecule catalyses a carbodiimide-to-urea fuel-to-waste reaction,[39–41] transiently forming an anhydride in which the motor accesses a different set of conformational dynamics to those available in the diacid state. Use of a chiral carbodiimide and a chiral hydrolysis promoter introduces kinetic asymmetry in the chemomechanical cycle,[14–16] resulting in continuous directionally biased 360° rotation of the rotor about the stator. We wondered if such a structurally simple catalysis-driven rotary motor could be incorporated into a soft matter matrix and used to explore mechanical work being done, and chemical energy transduced, by motor-molecule catalysis (Fig. 1c).

Motor **1** (Fig. 1a) is an analogue of the previously reported rotary motor,[10] derivatised with terminal alkynes extending from the 4- and 5- positions of the stator and 3- and 4-positions of the rotor to allow the motor's attachment to azide-terminated polymers through copper-mediated azide–alkyne 'click' cycloaddition[42] (Supplementary Information, Section S2). Fuelling **1** with diisopropylcarbodiimide (DIC)[12,31,34,39,40] in the presence of 4-dimethylaminopyridine (DMAP) resulted in transient anhydride formation (Supplementary Information, Section S4.1), indicating that the key acid-to-anhydride-to-acid chemical transformations in the chemomechanical cycle[10,31,34] of the motor are unaffected by the additional functionalisation.

Tetra-alkyne **1** was treated with bisazide-terminated polyethylene glycol (PEG_{5000}, number average molecular weight (M_n) = 5000 g mol^{-1}), CuBr and *N*,*N*,*N*',*N*'',*N*''-pentamethyldiethylenetriamine (PMDETA) in CH_2Cl_2, forming gel-**1** through chemical crosslinking of the polymer chains at the motor nodes (Fig. 1a; Supplementary Information, Section S3.1).[36] Following removal of the copper salts and PMDETA by successive washings with CH_3CN and aqueous sodium ethylenediaminetetraacetate (Na_2-EDTA), gel-**1** was swollen in dioxane/H_2O (8:5, *v*/*v*). This solvent system balances the need to swell gel-**1** with the solubility of the chemical fuel and was used in all of the fuelling experiments reported in this study (see Supplementary Information, Sections S3.2 and S3.3).

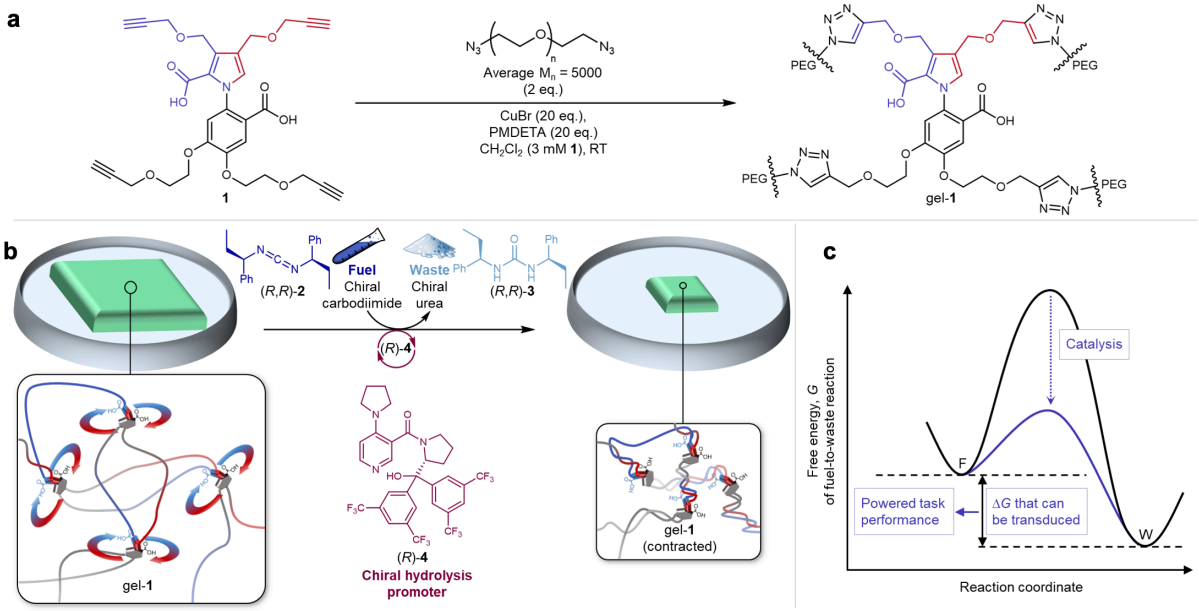

Fig. 1 | Contraction of a polymer gel with a covalently embedded chemically fuelled molecular motor. a, Chemical structure of motor **1** and its conversion into a cross-linked gel (gel-**1**) with motor units at the reticulation nodes, through copper(I)-catalysed azide-alkyne cycloaddition (CuAAC) with azide-terminated PEG chains. **b**, Treatment of gel-**1** with chiral fuel (*R*,*R*)-**2** and chiral hydrolysis promoter (*R*)-**4** leads to directional rotation of the motor components through the motor's catalysis of carbodiimide-to-urea hydration[12]. This winds the polymer chains around each other, increasing writhe, creating new physical entanglements, and causing the gel to contract. The (*R*,*R*)-**2** and (*R*)-**4** fuelling system causes biased clockwise rotation of the motor components, increasing writhe in a (+)-helical sense in the polymer strands. **c**, Transduction of chemical energy by catalysis of a fuel (F) to waste (W) reaction by a molecular ratchet. The energy available for transduction depends on the chemical potential difference between the fuel and waste and the kinetic asymmetry of the chemical engine cycle[6].

A racemic model diacid (±)-**5**,[10] which cannot fully rotate and so exists as enantiomeric atropisomers, was treated with chiral carbodiimide (*R*,*R*)-**2** and hydrolysis promoter (*R*)-**4**, producing urea (*R*,*R*)-**3** (Fig. 2a). The organocatalysis reaction resulted in a 40% enantiomeric excess of (+)-**5**, confirming that the chiral fuelling system generates similar directional rotational bias in the chemical engine cycle to the previous catalysis-driven motor-molecule[10] (Fig. 2b; Supplementary Information, Section S4.2). We next confirmed that gel-**1** was able to catalyse carbodiimide-to-urea hydration[12] with an efficacy similar to that of the monomeric motor (Fig. 2b; Supplementary Information, Section S4.3). These experiments demonstrated that (i) the diffusion of the fuelling reagents within the gel is not rate limiting;[43] (ii) the rotary motors at the reticulation nodes of the swollen gel are accessible to the chemical fuel; and, (iii), when covalently embedded in the gel, motor **1** retains the ability to function as a catalyst for the fuel-to-waste reaction.[10,41]

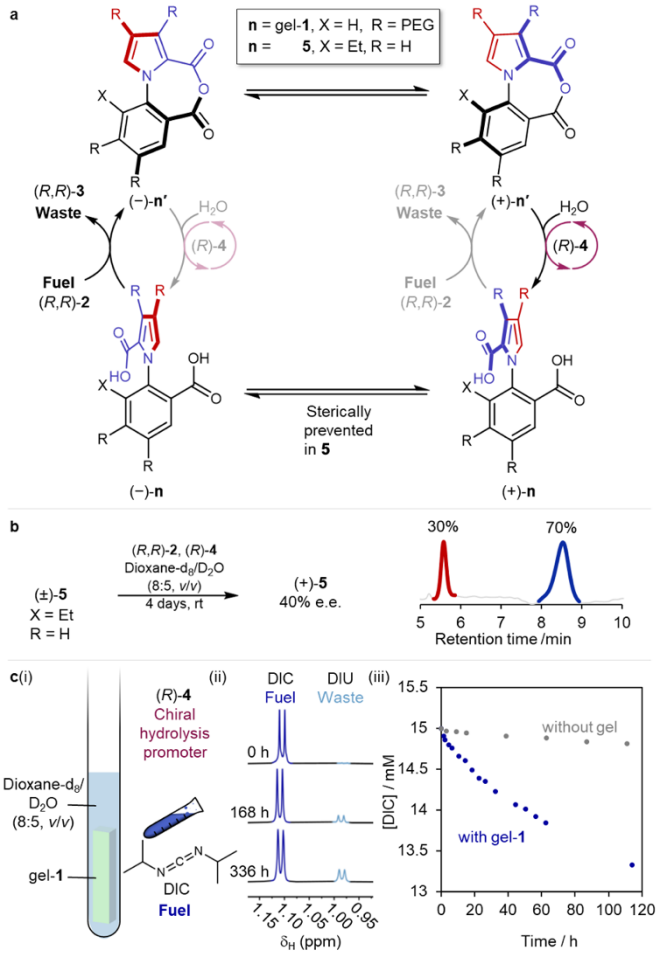

Fig. 2 | Directional bias and catalytic efficacy of gel-1 and model compounds. a, Mechanism of repetitive directionally biased 360° rotation of motor units in gel-**1** and of the deracemisation of motor model (±)-**5** with (*R*,*R*)-**2** and (*R*)-**4** under the fuelling conditions used for the gel experiments (dioxane-d_8/D_2O (8:5, *v*/*v*)). **b**, Chiral HPLC (ChiralPak-IF column, 25 °C, CH_2Cl_2:*i*-PrOH:CF_3CO_2H (95:5:0.1, *v*/*v*/*v*)) analysis showing 40% e.e. deracemisation of **5** under these fuelling conditions (Supplementary Information, Section S4.2); a directional bias of 2.3:1 clockwise:anti-clockwise rotation (i.e. a 'mistake' is made in directional rotation every 3 or 4 turns[10]). **c**, (i) Catalysis of a carbodiimide-to-urea fuel-to-waste reaction by gel-**1** (Supplementary Information, Section S4.3). (ii) Partial ^{1}H NMR spectra (dioxane-d_8/D_2O (8:5, *v*/*v*), 600 MHz, 298 K) showing progression of the fuel-to-waste reaction. Diisopropylcarbodiimide (DIC) was used as the fuel in this experiment as the ^{1}H NMR resonances of DIC and diisopropylurea (DIU) used to monitor the reaction do not overlap with those of gel-**1**. (iii) Plot of the consumption of DIC fuel for the uncatalysed (grey) and gel-**1**-catalysed (blue) reactions, showing catalysis of the fuel-to-waste reaction by gel-**1**.

With an appropriate chemical fuelling protocol established, a thin square of gel-**1** (dimensions ~10×10×1 mm; ~0.08 mmol motor units) was treated with a solution of the chiral hydrolysis promoter (*S*)-**4** (4 mmol, 50 equiv.) in dioxane/H_2O (8:5, *v*/*v*) at room temperature. The addition of (*S*)-**4** caused an expansion of the gel (~10%) associated with diffusion-driven swelling[44] and a likely change in protonation state of the motor as (*S*)-**4** is basic (Supplementary Information, Section S5.4.1). Only once the size of the gel was stable (4 h after addition of (*S*)-**4**) was fuelling begun (*t* = 0, Fig. 3d) by adding chiral carbodiimide (*S*,*S*)-**2** (8 mmol, 100 equiv.) in dioxane/H_2O (8:5, *v*/*v*) (Fig. 3a; Supplementary Information, Section S5.3). Contraction of the gel then occurred over 7 days (Fig. 3d, blue trace; Supplementary Video S1 & S2), resulting in a ~30% contraction of the gel (determined by measuring the surface area decrease of the gel and assuming an isotropic effect on volume, Fig. 3d, equation 1;[38] Supplementary Information, Section S5.2). Even after the gel stopped contracting, catalysis of

carbodiimide hydration by the gel-embedded motors continued as long as unreacted fuel remained or if the fuel was replenished.

A dimethyl ester derivative of the gel, gel-**1**-Me_2, in which the carboxylic acid groups of the motor are methylated and so are unable to catalyse hydration of the fuel (Fig. 3b), displayed similar swelling when treated with (*S*)-**4** but no contraction after the addition of (*S*,*S*)-**2** (Supplementary Video S6 and Supplementary Information, Section S5.4.3).

The rheology of gel-**1** was compared before and after fuelling with (*S*,*S*)-**2** and (*S*)-**4** (Fig. 4a; Supplementary Information, Section S6). The storage modulus (G′) of the gel was measured and found to be 2–3 orders of magnitude higher than the loss modulus (G″) in the measurability limit below 10 Pa. For both the unfuelled and fuel-contracted gel, G′ is constant across the whole frequency range (Fig. 4a), which is typical for polymer gels at low frequency in the hydrodynamic regime. The storage modulus is proportional to the number of crossings multiplied by the elastic energy per chain, so the 4.6-fold increase in G′ (0.3 kPa unfuelled; 1.4 kPa fuel-contracted) indicates that an increase in the number of strand entanglements in the gel occurs as a result of fuelling.[45,46] This macroscopic measurement is a direct consequence of the twisting of the polymer chains around each other by catalysis-driven motor rotation at the nanoscale.

Effects attributable to the twisting of the polymer strands in the gel were also evident at the microscopic scale (Supplementary Information, Section S6). Atomic force microscopy (AFM) images of the gel surface show changes in polymer chain conformation, with the appearance of numerous kinks after contraction (Fig. 4b) reflecting an increase in writhe. The reduction in surface homogeneity and the appearance of larger pores in the gel after fuelling (Fig. 4b) can be attributed to the action of the winding of the polymer chains around one another generating large spaces empty of material in between denser, highly entangled, regions.[36]

These experiments all indicate that the macroscopic contraction of gel-**1** under fuelling with the chiral carbodiimide is a result of the organocatalysis-driven directional rotation of the motor-molecules increasing the entanglement (writhe[47]) of the polymer strands within the gel.[36,48]

From the directionality obtained from fuelling (±)-**5** (Fig. 2b), the directional rotation of the motor is clockwise with the (*S*,*S*)-**2** and (*S*)-**4** fuelling system, generating (−)-writhe in the polymer chains of gel-**1**. Fuelling of a pristine sample of gel-**1** with reagents of the opposite chirality, i.e. (*R*,*R*)-**2** and (*R*)-**4**, caused gel contraction with a similar rate and profile (Fig. 3d, red trace; Supplementary Video S3 & S4) to the (*S*,*S*)-**2** and (*S*)-**4** fuelling system. Anti-clockwise rotation of the motor-molecules results in twisting of the polymer strands to introduce writhe with a positive helical twist-sense. However, fuelling a sample of gel-**1** with an achiral fuelling system (DIC and 4-dimethylaminopyridine (DMAP)) led to no contraction of the gel, despite efficient catalysis of the fuel-to-waste reaction by the gel-embedded motors (Supplementary Video S5; Supplementary Information, Section S5.4.2).

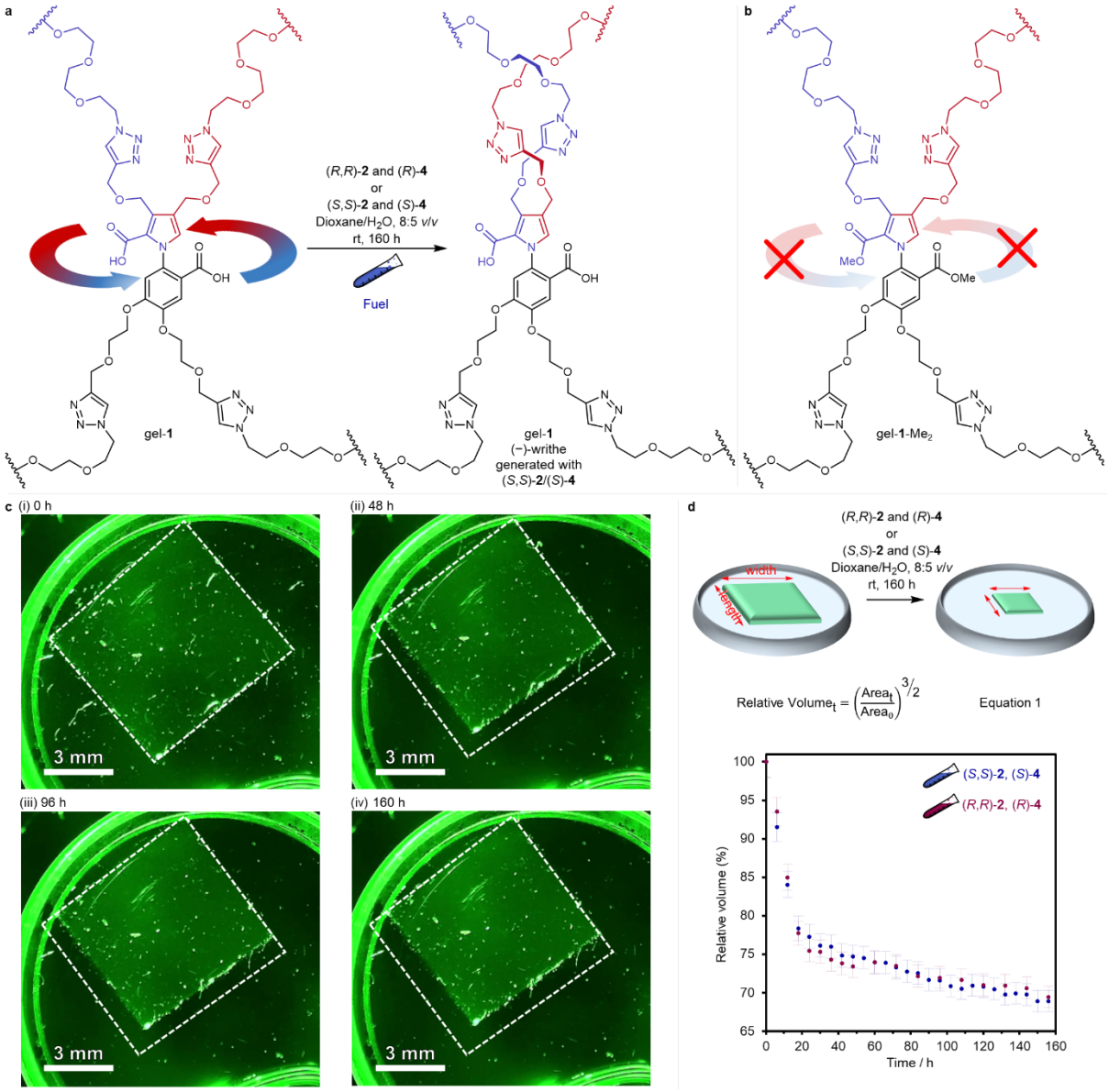

Fig. 3 | Macroscopic contraction of gel-1 under chemical fuelling. a, Directional rotation of the rotor about the stator during catalysis by the motors embedded in gel-**1** results in twisting of the polymer chains, inducing writhe (additional strand crossings); Supplementary Videos S1–S4. **b**, The motor-molecules in the methyl ester control gel-**1**-Me_2 are unable to catalyse the fuel-to-waste reaction (nor can the methyl groups rotate past each other) and therefore do not directionally rotate under chemical fuelling (Supplementary Video S6; Supplementary Information, Section S5.4.3). **c**, Images of gel-**1** during chemically fuelled contraction with (*S*,*S*)-**2** and (*S*)-**4** (Supplementary Video S1 & S2) at (i) 0 h, (ii) 48 h, (iii) 96 h and (iv) 160 h. The white dashed line shows the outline of the gel prior to fuelling (t = 0). **d**, Contraction of gel-**1** under chemical fuelling. Equation 1 gives the decrease in volume (assuming isotropic contraction) based on the change in area of the horizontal face of the gel (moulded and then cut to the shape of a rectangular prism), pictured from above (gel area measured by image analysis with ImageJ; Supplementary Information, Section S5.2). The change in %volume was plotted over time, with contraction continuing under fuelling for 7 days. Fuelling carried out with (i) (*S*,*S*)-**2** and (*S*)-**4** (blue data points) or (ii) (*R*,*R*)-**2** and (*R*)-**4** (red data points).

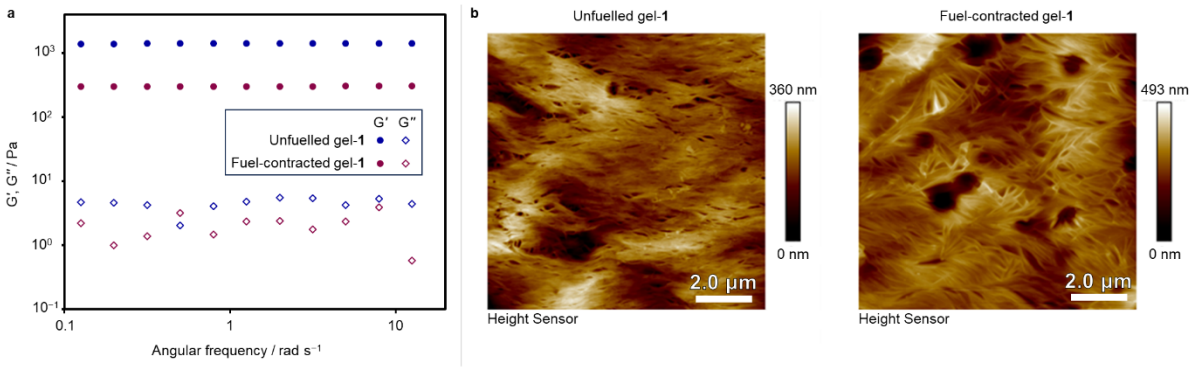

Fig. 4 | Rheological and atomic force microscopy comparison of gel-1 before and after chemically fuelled contraction. a, Variation of G' (storage modulus) and G'' (loss modulus) before and after gel contraction, as a function of angular frequency (Supplementary Information, Section S6). **b**, AFM images of gel-**1** before and after fuelled contraction (Supplementary Information, Section S6).

The point at which gel contraction stops in the chiral fuelling experiments, despite fuel remaining and catalysis continuing, corresponds to the unravelling force exerted by the twisted polymer strands and the osmotic pressure from gel contraction, equalling the directional bias for rotation of the motor-molecules under catalysis. This is the stall force, a typical performance measure of motor proteins.[1–3] How motor proteins respond to an applied force in chemical and conformational terms is often difficult to deconvolute clearly. However, because the mechanism of catalysis of the fuel-to-waste reaction by **1** is a well-defined series of steps, here it is apparent what the stall force corresponds to in terms of a chemomechanical mechanism. The directionality of rotation of **1** under catalysis (the ratcheting constant, K_r,[11] or Astumian's 'r_0'[3]) arises from the Curtin–Hammett asymmetry factor ($F_{C–H}$) of the motor.[7] This is determined by the two Curtin–Hammett-type kinetic resolutions in the reaction cycle shown in Fig. 2a. The force exerted by the twisted polymer strands will affect the bias in the conformational exchange processes ((−)-**1**⇋(+)-**1** and (−)-**1**'⇋(+)-**1**', Fig. 2a). The stall force corresponds to the point where $F_{C–H}$ = 1. This would be reached when the ratios [(−)-**1**]:[(+)-**1**] and [(−)-**1**']:[(+)-**1**'], which are both 1:1 for the pairs of enantiomeric conformers in the absence of force, are driven away from 1:1 by the applied force such that at the stall force they balance the Curtin–Hammett effect.

Once the fuel supply is exhausted, the motor-molecules are kinetically locked in the diacid state and the gel remains contracted (no relaxation/re-expansion of the gel occurs over the course of several months). However, the ability to select the direction of rotation of the motors according to the handedness of the fuel allows the macroscopic gel contraction to be reversed by powered unwinding of the polymer chains (Fig. 5; Supplementary Video S7 & S8; Supplementary Information, Section S5.5).

A sample of gel-**1** was contracted to ~70% of its original size by fuelling with (*S*,*S*)-**2** and (*S*)-**4** to cause anti-clockwise rotation and induce (−)-twists in the polymer strands (Fig. 5c, blue data points 0–160 h). The resulting (−)-writhe-contracted-gel was then washed extensively to remove waste and residual fuel and reagents, resulting in a further reduction in the volume of the now-'empty' (−)-writhe-contracted-gel to 61% of its original size (Fig. 5c; red data point at 0 h of second fuelling). The (−)-writhe-contracted-gel was then re-swollen in dioxane/water (8:5, *v*/*v*) and (*R*,*R*)-**2** and (*R*)-**4** added to power catalysis-driven rotation of the gel-embedded-motors in the opposite direction (i.e., clockwise). Under this fuelling

regime, the (−)-writhe-contracted-gel first expanded over 5 h from the 61% minimum volume to a maximum of 81% of the original gel size (Fig. 5c, red data points). ~10% of this expansion can be attributed to diffusion-driven swelling from addition of the new batch of fuel and hydrolysis promoter, but much more modest expansion in control experiments (second fuellings with (*S*,*S*)-**2**/(*S*)-**4** or DIC/DMAP; Supplementary Information Section 5.5; Supplementary Video S9) indicates that the substantial expansion results from powered clockwise unwinding of the anti-clockwise twisted polymer strands. After the maximum size of the gel is reached under fuelling with the (*R*,*R*)-**2** and (*R*)-**4** fuelling system (5 h, red data points, Fig. 5c), rotation of the motors under catalysis continues in the clockwise direction and the gel begins to contract again, reaching a minimum volume of 62% after 60 h of fuelling with (*R*,*R*)-**2** and (*R*)-**4** (Fig. 5c, red data points; Supplementary Video S7 & S8, Supplementary Information, Section S5.5).

The original volume of the gel is not fully recovered by the powered expansion (Fig. 5c, red data points). This is expected as the originally twisted strands will not all become fully unwound at the same time. Once an anticlockwise-twisted strand-pair becomes fully unwound by the now-clockwise-rotating motor, that strand-pair will continue to be twisted clockwise by the motor, winding those strands around each other again before some of the other, anti-clockwise-twisted, strand-pairs in the gel have been fully unwound. As such, powered directional rotation-mediated expansion does not return the gel to its original equilibrium state, but rather drives the gel from one out-of-equilibrium state to another.

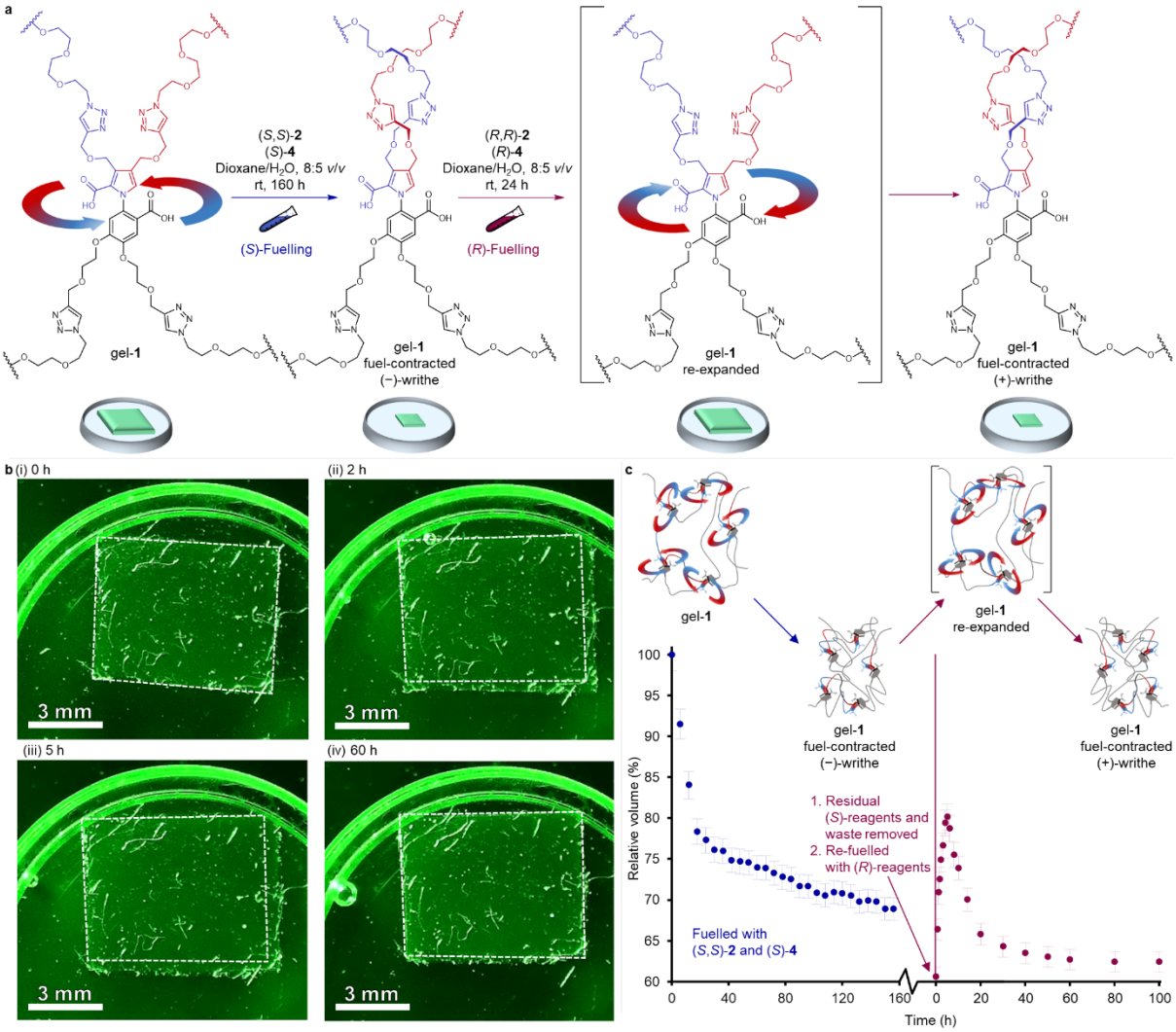

Fig. 5 | Chemically fuelled expansion–re-contraction of a sample of fuel-contracted gel-1 (Supplementary Information, Section S5.5). **a**, A gel sample that had been contracted with (*S*,*S*)-**2** and (*S*)-**4** and then exhaustively washed to remove waste and residual fuel, was then treated with (*R*,*R*)-**2** and (*R*)-**4** (i.e., the fuelling system of opposite chirality) to power rotation of the motor components in the opposite direction. This first powered untwisting of the polymer strands, causing expansion of the previously contracted gel (*t* = 0-to-5 h of the red data points, Fig. 5c), after which the catalysis-driven rotation began to re-introduce writhe of the opposite twist-sense. **b**, Images of gel-**1** during this chemically fuelled expansion-contraction (Supplementary Video S7 & S8) at (i) 0 h, (ii) 2 h, (iii) 5 h and (iv) 60 h. The white dashed line shows the outline of the contracted gel prior to the second fuelling (*t* = 0 of red data points). **c**, The change in %volume plotted over time showing the powered contraction–expansion–contraction behaviour of gel-**1** upon successive fuelling with systems of the opposite chirality (blue data points (*S*,*S*)-**2** and (*S*)-**4**; red data points (*R*,*R*)-**2** and (*R*)-**4**).

Current generations of artificial chemically (e.g., pH) responsive gels and polymers used for actuation operate through switching.[49–51] In contrast, the motor-molecule units in gel-**1** generate force by fuelling biasing the kinetics of ground-state conformational changes, the same type of catalysis-driven information ratchet mechanism as biological motor-molecules. In doing so, work is accumulated; each turn of a motor progressively adding to the force generated and work done. This is fundamentally different to switching, where any work done by the change in state of the switch is undone by a full operating cycle.[16,51–54] The generation of force and performing of work by gel-**1** is reminiscent of myosin II, the motor protein that powers muscle contraction in most animal cells[3,8,9] (although gel-**1** acts through

rotary rather than linear molecular-level dynamics). Myosin II is a hexameric protein with a molecular mass of 450 kD, whereas each organocatalytic motor unit in gel-**1** consists of just 17 non-hydrogen atoms. Nevertheless, in both cases the action of catalysis causes force to be generated and work to be done by the catalyst transducing chemical energy from the catalysed reaction to mechanical energy and elastic energy storage (Fig. 1c). The simplicity of the synthetic system means that the chemomechanical mechanism by which this happens is clearly apparent. As both key conformational changes in the ratcheting cycle occur between enantiomeric atropisomers ((+)-**1** and (−)-**1**; (+)-**1**' and (−)-**1**'), there is no power stroke. The experimental demonstration of the transduction of chemical energy to perform work against a load through kinetic asymmetry provides a minimalist mechanistic illustration of how catalysis-driven molecular motors can extract order from chaos[4].

Data availability

The data that support the findings of this study are available within the paper and its Supplementary Information, or are available from the Mendeley data repository (https://data.mendeley.com/) at http://xxxxx

Acknowledgements

The authors thank Dr B. M. W. Roberts for useful discussions and the analytics platforms of Institut Charles Sadron and Mounir Maaloum for physical characterisation of the Information. This work was funded by the Engineering and Physical Sciences Research Council (EPSRC; EP/P027067/1), the European Commission's Horizon 2020 Programme, through the Marie Sklodowska-Curie Action–Innovative Training Network (MSCA-ITN) project ArtMoMa (grant no. 860434) and the European Research Council (Advanced grant 786630). We thank the China Scholarship Council (CSC, file no. 202108310032) and the University of Manchester for a PhD studentship to P.-L.W. D.A.L. is a Royal Society Research Professor.

Author contributions

P.-L.W., S.B. and D.A.L. conceived the project. P.-L.W. synthesised the motor and carried out the gel contraction experiments. M.J.P. assisted with gel formation and contraction experiments. A.C. showed P.-L.W. and M.J.P. how to make suitable gels and performed the AFM and rheology measurements. D.A.L., S.B. and N.G. directed the research. P.-L.W., M.J.P., S.B. and D.A.L. wrote the paper with input from N.G. and A.C.

Competing interests

The authors declare no competing interests.

Supplementary Information The online version contains supplementary material available at xxxxx.

Correspondence and requests for Information should be addressed to David A. Leigh or Nicolas Giuseppone.

References

1. Schliwa, M. & Woehlke, G. Molecular motors. *Nature* **422**, 759–765 (2003).

2. Howard, J. Protein power strokes. *Curr. Biol.* **16**, R517 (2006).

3. Astumian, R. D. Irrelevance of the power stroke for the directionality, stopping force, and optimal efficiency of chemically driven molecular machines. *Biophys. J.* **108**, 291–303 (2015).

4. Hoffmann, P. W. How molecular motors extract order from chaos (a key issues review). *Rep. Prog. Phys*. **79**, 032601 (2016).

5 Hwang, W. & Karplus, M. Structural basis for power stroke vs. Brownian ratchet mechanisms of motor proteins. *Proc. Natl. Acad. Sci. U.S.A.* **116**, 19777–19785 (2019).

6. Amano, S., Borsley, S., Leigh, D. A. & Sun, Z. Chemical engines: driving systems away from equilibrium through catalyst reaction cycles. *Nat. Nanotechnol.* **16**, 1057–1067 (2021).

7. Amano, S. et al. Using catalysis to drive chemistry away from equilibrium: relating kinetic asymmetry, power strokes and the Curtin–Hammett principle in Brownian ratchets. *J. Am. Chem. Soc*. **144**, 20153–20164 (2022).

8. Sweeney, H. L. & Houdusse, A. Structural and functional insights into the myosin motor mechanism. *Annu. Rev. Biophys.* **39**, 539–557 (2010).

9. Irving, M. et al. Conformation of the myosin motor during force generation in skeletal muscle. *Nat. Struct. Biol.* **7**, 482–485 (2000).

10. Borsley, S., Kreidt, E., Leigh, D. A. & Roberts, B. M. W. Autonomous fuelled directional rotation about a covalent single bond. *Nature* **604**, 80–85 (2022).

11. Ragazzon, G. & Prins, L. J. Energy consumption in chemical fuel-driven self-assembly. *Nat. Nanotechnol.* **13**, 882–889 (2018).

12. Schwarz, P. S., Tena-Solsona, M., Daia, K. & Boekhoven, J. Carbodiimide-fuelled catalytic reaction cycles to regulate supramolecular processes. *Chem. Commun.* **58**, 1284–1297 (2022).

13. Aprahamian, I. & Goldup, S. M. Non-equilibrium steady states in catalysis, molecular motors, and supramolecular Information: Why networks and language matter. *J. Am. Chem. Soc*. **145**, 14169–14183 (2023).

14. Sangchai, T., Al Shehimy, S., Penocchio, E. & Ragazzon, G. Artificial molecular ratchets: tools enabling endergonic processes. *Angew. Chem. Int. Ed.* **62**, e202309501 (2023).

15. Astumian, R. D. Kinetic asymmetry and directionality of nonequilibrium molecular systems. *Angew. Chem. Int. Ed.* **63**, e202306569 (2024).

16. Borsley, S., Leigh, D. A. & Roberts, B. M. W. Molecular ratchets and kinetic asymmetry: Giving chemistry direction. *Angew. Chem. Int. Ed.* **63**, e202400495 (2024).

17. Koumura, N., Zijlstra, R. W. J., van Delden, R. A., Harada, N. & Feringa, B. L. Light-driven monodirectional molecular rotor. *Nature* **401**, 152–155 (1999).

18. Leigh, D. A., Wong, J. K. Y., Dehez, F. & Zerbetto, F. Unidirectional rotation in a mechanically interlocked molecular rotor. *Nature* **424**, 174–179 (2003).

19. Guentner, M. et al. Sunlight-powered kHz rotation of a hemithioindigo-based molecular motor. *Nat. Commun*. **6**, 8406 (2015).

20. Wilson, M. R. et al. An autonomous chemically fuelled small-molecule motor. *Nature* **534**, 235–240 (2016).

21. Erbas-Cakmak, S. et al. Rotary and linear molecular motors driven by pulses of a chemical fuel. *Science* **358**, 340–343 (2017).

22. Pumm, A.-K. et al. A DNA origami rotary ratchet motor. *Nature* **607**, 492–498 (2022).

23. Zhang, L. et al. An electric molecular motor. *Nature* **613**, 280–286 (2023).

24. Berreur, J., Watts, O. F. B., Bulless, T. H. N., O'Donoghue, N. T., Winter, A. J., Clayden, J. & Collins, B. S. L. Redox-powered autonomous unidirectional rotation about a C–C bond under enzymatic control, ChemRxiv (2024); doi:10.26434/chemrxiv-2024-tz8vc.

25. Serreli, V., Lee, C.-F., Kay, E. R. & Leigh, D. A. A molecular information ratchet. *Nature* **445**, 523–527 (2007).

26. Ragazzon, G., Baroncini, M., Silvi, S., Venturi, M. & Credi, A. Light-powered autonomous and directional molecular motion of a dissipative self-assembling system. *Nat. Nanotechnol*. **10**, 70–75 (2015).

27. Cheng, C. et al. An artificial molecular pump. *Nat. Nanotechnol.* **10**, 547–553 (2015).

28. Qui, Y. et al. A precise polyrotaxane synthesizer. *Science* **368**, 1247–1253 (2020).

29. Feng, L. et al. Active mechanisorption driven by pumping cassettes. *Science* **374**, 1215–1221 (2021).

30. Amano, S., Fielden, S. D. P. & Leigh, D. A. A catalysis-driven artificial molecular pump. *Nature* **594**, 529–534 (2021).

31. Borsley, S., Leigh, D. A. & Roberts, B. M. W. A doubly kinetically-gated information ratchet autonomously driven by carbodiimide hydration. *J. Am. Chem. Soc.* **143**, 4414–4420 (2021).

32. Thomas, D. et al. Pumping between phases with a pulsed-fuel molecular ratchet. *Nat. Nanotechnol.* **17**, 701–707 (2022).

33. Corra, S. et al. Kinetic and energetic insights into the dissipative non-equilibrium operation of an autonomous light-powered supramolecular pump. *Nat. Nanotechnol*. **17**, 746–751 (2022).

34. Binks, L. et al. The role of kinetic asymmetry and power strokes in an information ratchet. *Chem* **9**, 2902–2917 (2023).

35. García-López, V. et al. Molecular machines open cell membranes. *Nature* **548**, 567–572 (2017).

36. Li, Q. et al. Macroscopic contraction of a gel induced by the integrated motion of light-driven molecular motors. *Nat. Nanotechnol.* **10**, 161–165 (2015).

37. Foy, J. T. et al. Dual-light control of nanomachines that integrate motor and modulator subunits. *Nat. Nanotechnol.* **12**, 540–545 (2017).

38. Perrot, A. Wang, W.-Z., Buhler, E., Moulin, E. & Giuseppone, N. Bending actuation of hydrogels through rotation of light-driven molecular motors. *Angew. Chem. Int. Ed.* **62**, e202300263 (2023).

39. Tena-Solsona, M. et al. Non-equilibrium dissipative supramolecular Information with a tunable lifetime. *Nat. Commun.* **8**, 15895 (2017).

40. Kariyawasam, L. S. & Hartley, C. S. Dissipative assembly of aqueous carboxylic acid anhydrides fuelled by carbodiimides. *J. Am. Chem. Soc.* **139**, 11949–11955 (2017).

41. Borsley, S., Leigh, D. A. & Roberts, B. M. W. Chemical fuels for molecular machinery. *Nat. Chem.* **14**, 728–738 (2022).

42. Liang, L. & Astruc, D. The copper(I)-catalyzed alkyne–azide cycloaddition (CuAAC) 'click' reaction and its applications. An overview. *Coord. Chem. Rev.* **255**, 2933–2945 (2011).

43. Hagel, J., Haraszti, T. & Boehm, H. Diffusion and interaction in PEG-DA hydrogels. *Biointerphases* **8**, 36 (2013).

44. Yavari, N. & Azizian, S. Mixed diffusion and relaxation kinetics model for hydrogels swelling. *J. Mol. Liq.* **363**, 119861 (2022).

45. Goujon, A. et al. Bistable [c2] daisy chain rotaxanes as reversible muscle-like actuators in mechanically active gels. *J. Am. Chem. Soc.* **139**, 14825–14828 (2017).

46. Colard-Itté, J.-R. Et al. Mechanical behaviour of contractile gels based on light-driven molecular motors. *Nanoscale* **11**, 51975202 (2019).

47. Ashbridge, Z. et al. Knotting matters: orderly molecular entanglements. *Chem. Soc. Rev.* **51**, 7779–7809 (2022).

48. Baiesi, M., Orlandini, E. & Whittington, S. G. Interplay between writhe and knotting for swollen and compact polymers. *J. Chem. Phys.* **131**, 154902 (2009).

49. Hu, L., Zhang, Q., Li, X. & Serpe, M. J. Stimuli-responsive polymers for sensing and actuation. *Mater. Horiz*. **6**, 1774–1793 (2019).

50. Liu, J., Jiang, L., He, S., Zhang, J. & Shao, W. Recent progress in PNIPAM-based multi-responsive actuators: A mini-review. *Chem. Eng. J*. **433**, 13349670 (2022).

51. Howse, J. R., Topham, P., Crook, C. J., Gleeson, A. J., Bras, W., Jones, R. A. L. & Ryan, A. J. Reciprocating power generation in a chemically driven synthetic muscle. *Nano Lett*. **6**, 73–77 (2006).

52. Chatterjee, M. N., Kay, E. R. & Leigh, D. A. Beyond switches: ratcheting a particle energetically uphill with a compartmentalized molecular machine. *J. Am. Chem. Soc*. **128**, 4058–4073 (2006).

53. Boekhoven, J., Hendriksen, W. E., Koper, G. J. M., Eelkema, R. & van Esch, J. H. Transient assembly of active Information fueled by a chemical reaction. *Science* **349**, 1075–1079 (2015).

54. Bruns, C. J. Moving forward in the semantic soup of artificial molecular machine taxonomy. *Nat. Nanotechnol*. **17**, 1231–1234 (2022).